Improved manufacturing process for printed cantilevers by using water removable sacrificial substrate

Almudena Rivadeneyra [a], José Fernández-Salmerón [a], Manuel Agudo-Acemel [b], Juan A. López-Villanueva [c], Luis Fermín Capitan-Vallvey [b], Alberto J. Palma [c,*]

[a] Institute for Nanoelectronics, Technische Universität München, DE-80333 Munich, Germany
[b] ECsens, Departamento de Química Analítica, Facultad de Ciencias Universidad de Granada, E-18071 Granada, Spain
[c] ECsens, Departamento de Electrónica y Tecnología de Computadores, ETSIIT Universidad de Granada, E-18071 Granada, Spain

A B S T R A C T

Suspended structures are an important element in the vast majority of electromechanical systems. The definition of this kind of structures is a not totally resolved problem in printing electronics where the definition of a smooth sacrificial layer makes difficult their fabrication. Based on a previous work using a sacrificial substrate, we present in this paper a significant improvement of this technique in terms of reproducibility and yield rate. The sacrificial substrate is a commercial polyvinyl alcohol film which can be removed by water. The structural material is silver paste which has shown better performance during the removal of the sacrificial substrate than the previous approach based on an acetone bath. Furthermore, this sacrificial material is biodegradable as well as its solvent. In this paper, we show the fabrication process for printed cantilevers, including a characterization of their peak to peak displacements as a function of the applied acceleration and frequency. Moreover, the variation of the capacitance for different acceleration values is presented.

1. Introduction

Suspended mechanical structures are useful in many different applications such as accelerometers, pressure sensors, actuators or fluidic devices [1]. Traditionally, these structures have been manufactured with micro-electromechanical system (MEMS) fabrication techniques and integrated with CMOS technology [2]. With this regard, the deposition of a sacrificial layer to support and define the suspended part while manufacturing is essential. This layer is removed at the end of the fabrication process depending on the particular process that is being used. Although many different strategies and materials have been used to fabricate these suspended structures based on silicon MEMS technologies, there are other processing technology platforms such as printed electronics where this development is not so advanced yet.

The advantages of printed electronics such as low-cost equipment, flexible substrates, low-cost materials, degradability and biocompatibility, open a wide range of new applications for example, radio frequency identification (RFID) tags, smart clothing or flexible displays. This technology is based on traditional printing techniques, such as gravure, screen printing, flexography and inkjet printing [3]. Many advances have been achieved in devices such as organic light-emitting diodes (OLED), thin film transistors (TFT), solar cells and printed antennas [4,5] but there are still some aspects that should be improved in terms of performance and reliability.

Great efforts and very valuable achievements have been done to develop printed sensors, mainly chemical sensors, and bioelectronics, but limited developments have been achieved in mechanical suspended structures. One of these not-resolved aspects is suspended structures by using only printing techniques. The main problems to face with respect to surface micromachining process are the smoothness of the sacrificial layer, its removal process [6], the stability of the pillar on a plastic substrate and the roughness of the plastic film. The sacrificial layer has to be smooth to properly define another layer on top of it. In addition to this, the removal method should not affect the rest of the layers. The most common method to remove the sacrificial layer is the chemical bath. It is not easy to find suitable materials to act as sacrificial layer, whose solvents do not affect the structural materials. The mechanical properties of the structural material are fundamental to the stability of the suspended structure but, with respect to the flexible substrate, it results more complicated to maintain the suspended part when the substrate is not rigid.

* Corresponding author. Fax: +34 958242330.
E-mail addresses: arivadeneyratorres@nano.ei.tum.de (A. Rivadeneyra), jfsalmeron@nano.ei.tum.de (J. Fernández-Salmerón), magudo@ugr.es (M. Agudo-Acemel), jalopez@ugr.es (J.A. López-Villanueva), lcapitan@ugr.es (L.F. Capitan-Vallvey), ajpalma@ugr.es (A.J. Palma).

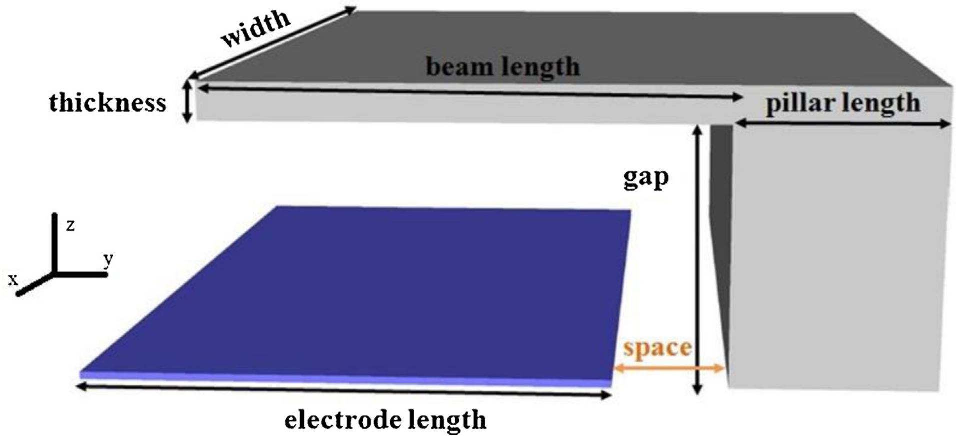

Fig. 1. Schematics of the cantilever.

Regarding the sacrificial layer, different strategies have been followed to reach these requirements. Lam et al. [7] used a poly(methyl methacrylate) (PMMA) sacrificial layer to develop a cantilever by screen printing with a releasing method based on chloroform baths followed by drying with a N_2 gun. Park et al. [8,9] also chose PMMA as sacrificial layer. PMMA was also chosen as sacrificial material by Chung et al. [10] to develop 4-terminal inverters. They removed the sacrificial layer by dipping into boiling acetone and isopropyl alcohol. This latter material was removed in an acetone bath to release a switch made by inkjet printing. Another used sacrificial layer has been a strontium carbonate ($SrCO_3$) in an epoxy-type ink which is dissolved by immersing the structure in a weak acidic solution [11,12]. Nathalie Serra et al. [6,13] employed a solution based on trimethylolethane removed by thermal treatment to develop bridges and cantilevers by screen printing. Another sacrificial layer used to manufacture bridges by inkjet printing was a commercial photoresist Microposit® 1813® from Shipley [14]. In this case, the sacrificial was removed by dissolving it in acetone. Shankar et al. [15] selected PMMA as sacrificial layer to develop ohmic contact RF MEMS switches and this layer was dissolved by soaking the structure in chloroform.

In regard to the used substrates, Fuller et al. [16] developed silver cantilevers on glass by inkjet printing. A silicon substrate was used by Park et al. [8] to fabricate printed switches and to develop 4-terminal inverters [10]. Wei et al. [17–21] fabricated piezoelectric cantilevers on cotton by screen printing. Alumina substrate has been chosen to manufacture suspended structures for several authors [6,12,13,22–24]. A few examples can also be found using plastic surfaces: a microelectromechamical switch developed on polyimide substrate by lamination techniques [25,26], switches on Kapton polyimide [15], electrostatic microactuators made of a flexible sheet [27], or printed bridges on polyethylene terephthalate (PET) [14] or a cantilever also developed on PET by screen printing [28]. In this previous work, the design, fabrication and characterization of a printed cantilever were reported.

Here, we present some advances in the fabrication of a printed cantilever on a plastic substrate. As described in our previous work [28], our fabrication process differs from others on the use of a commercial film, PMMA, as sacrificial material. The main difference remains in the role of this layer: it is also used as a substrate for printing the beams and the pillars, and then this substrate is flipped and bonded to the printed electrodes substrate. These electrodes had been previously printed on another substrate. After a bonding process, the sacrificial substrate is removed. The structure presented here are essentially made using the same process flow, but while in our previous work the sacrificial substrate had to be chemically etched, we have used now a different material so that it can be eliminated with a different solvent without virtually inferring with the structural material. Hence, while we stated that our previous process was similar to the wafer bonding procedure developed to obtain Silicon-On-Insulator wafers in microelectronic technology, this new procedure is similar to the Unibond™ method that does not require to etch the whole wafer [29]. An important advantage of this new procedure is that there is no degradation of any layer during the removal of the sacrificial substrate because it is a layer of transference. In addition to this, the substrate is a plastic substrate, which provides more flexibility to the final device but less stability during the manufacturing process of the suspended structures.

2. Materials and methods

2.1. Design

To design this structure, we have implemented the same approach we developed in our previous work [28] to directly compare results. Given the complicated geometry of the printed cantilever, we skipped the development of an analytical model and we directly used a multiphysics numerical simulator, COMSOL (Comsol Inc., Stockholm, Sweden), based on solving partial differential equations with the finite element method. This software has previously been used to calculate displacements and resonance

Table 1
Dimensions of the designed suspended structure.

Parameter	Value	Description
Length (mm)	5.0	Length of the beam
Width (mm)	2.5	Width of the beam
Gap (μm)	120	Distance between the back electrode and the beam (*z*-axis)
Space (mm)	1.0	Distance between the back electrode and the beam (*y*-axis)
Thickness (μm)	15	Thickness of the beam

Table 2
Comparison between numerical and experimental physical dimensions of the cantilever beams with PMMA layer and PVA layer.

Parameter	Model	Experimental PVA procedure	Experimental PMMA procedure [28]
Length (mm)	5.0	4.97 ± 0.05	4.98 ± 0.05
Width (mm)	2.5	2.56 ± 0.06	2.59 ± 0.05
Gap (μm)	120	125.7 ± 1.5	132 ± 2
Thickness (μm)	15	16.8 ± 0.1	17.3 ± 0.1
Capacitance (pF)	3.85	3.62 ± 0.01	3.51 ± 0.01

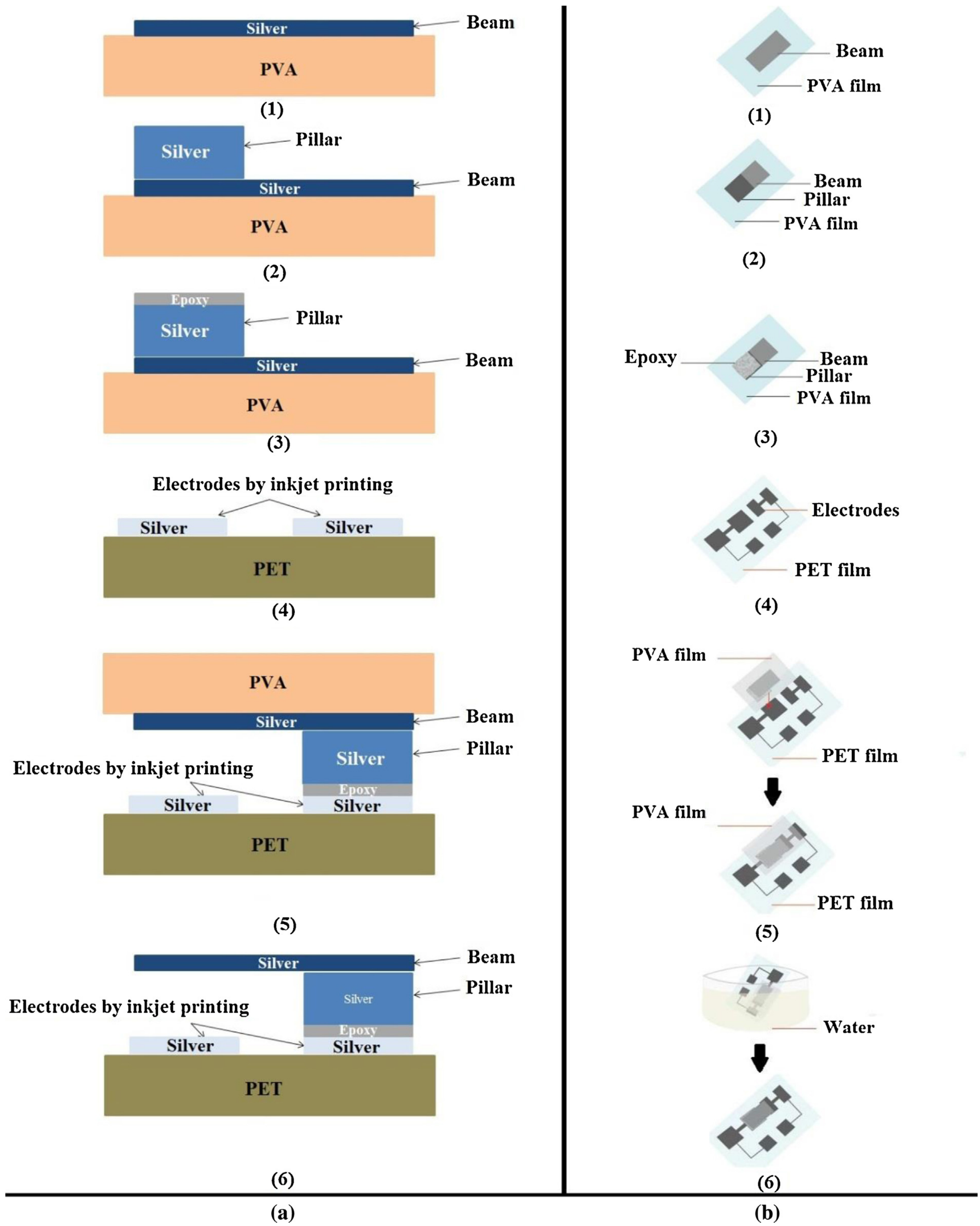

Fig. 2. Fabrication flow (a) Lateral view, (b) Top view.

frequencies in similar structures [30,31]. In order to simulate this structure, we followed the same procedure as explained in [28], using the electromechanical module. We performed several parametrical analyses to obtain a sensitivity of about 0.1 pF/g, where g is the gravity acceleration, a detectable value of capacitance in equilibrium of at least 1 pF, and a resonance frequency above 1 kHz to avoid fractures while oscillating. For this reason, we chose the dimensions shown in Table 1. Fig. 1 illustrates a *z*–*x* view of the cantilever.

In order to test the fabrication process, we also printed the same design of cantilever but we reduced the gap between the substrate and the suspended structure, from 120 μm to about 40 μm.

Fig. 3

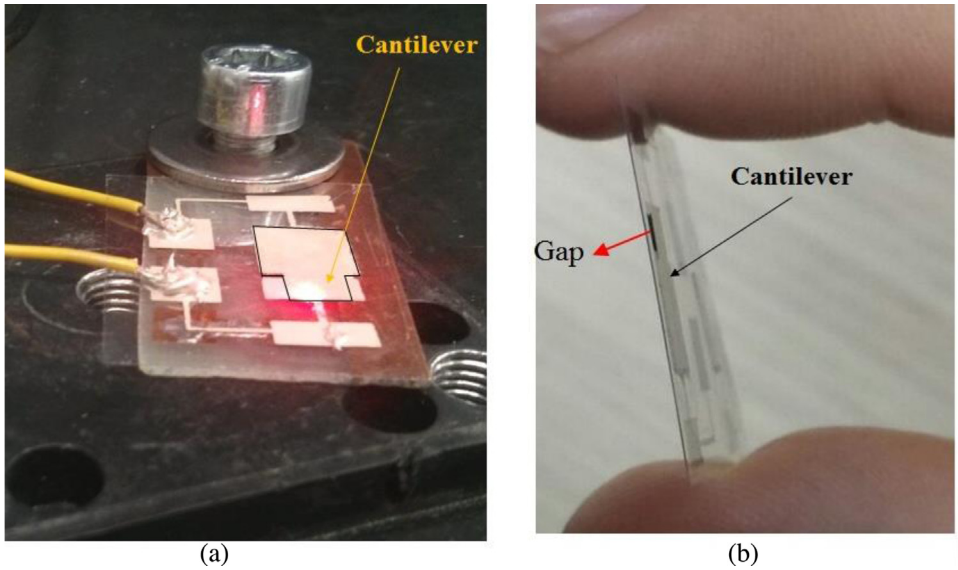

Fig. 3. Image of the screen printed cantilever (a) on the experimental set-up for displacement measurements; (b) lateral view of the cantilever.

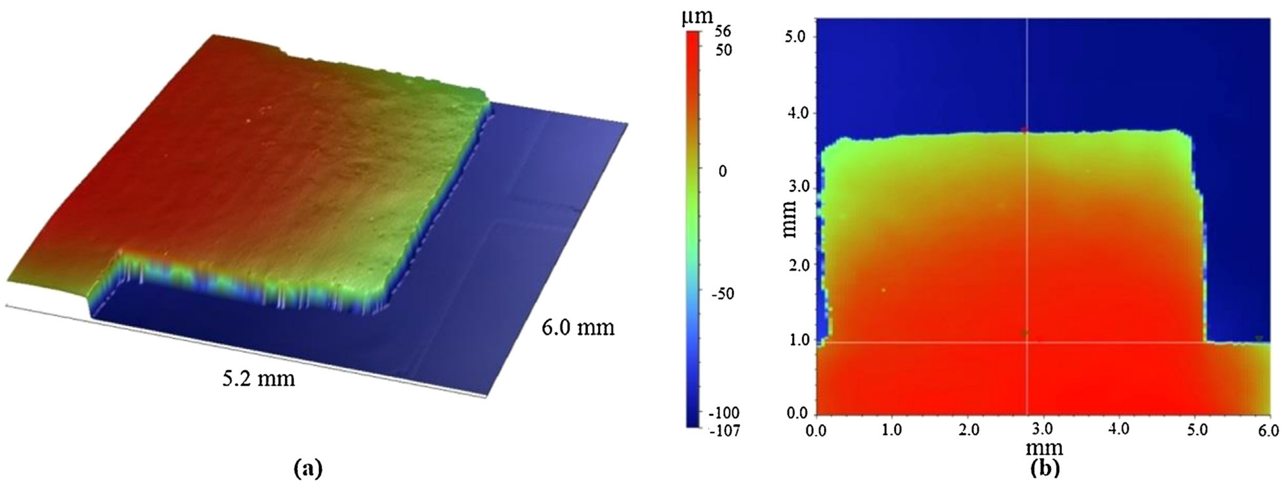

Fig. 4. Profiling system captions (a) 3D, (b) 2D.

2.2. Fabrication process

Although many of the steps needed to fabricate our printed cantilever are the same that were used in our previous work [28], we are detailing here the whole process flow. The cantilever was printed on a polyethylene terephthalate (PET) substrate of 75 μm thickness (ES301061 Goodfellow Cambridge Ltd., Huntingdon, UK) with a Serfix III screen printing machine (Seglevint SL, Barcelona, Spain). The alignment was performed with a semi-automatic pick and place system, ProtoPlace S from LPKF AG (LPKF Laser & Electronics AG, Garbsen, Germany) with a resolution of 500 μm. The screen used to manufacture the patterns by screen printing had a mesh density of 43 Nylon thread per centimetre (T/cm) in an aluminium rectangular structure of 50 cm in width and 35 cm in length. We chose this mesh density in order to reduce the number of printing layers to achieve the desired thickness of the structural material [32], finding a compromise between roughness and manufacturing time. The DMP-2831^{TM} Dimatix printer (Fujifilm Dimatix Inc, Santa Clara, USA) was used to print the electrodes. We decided to define them by inkjet printing because we only needed a thin layer to form the electrical contact to measure capacitance. They were made of silver nanoparticles (U5603 SunTronic Technology, San Diego, USA). The advantage of mixing these printing techniques is to achieve thicker patterns in the beam and pillar but not in the electrodes. Therefore, screen printing results more suitable for defining the pillar and the beam whereas inkjet printing is more convenient for the electrodes [32]. Anyway, only one printing technique would be enough to fabricate the structures with minimal modifications.

The structural materials of the cantilevers were conductive silver ink CRSN 2569 (Sun Chemical Corporation, Parsippany, USA) and epoxy EPO-TEK H20E (Epoxy Technology, Inc., Billerica, USA) because it allows to glue both printed parts and provide them electrical conductivity. The sacrificial substrate is a polyvinyl alcohol (PVA) film (MAVINSOL® available from Coemmo, Spain) of 50 μm thickness. This is one of the main innovations of our new structure over the previous one, which used PMMA as the sacrificial material, with the additional advantage of avoiding the destructive chemical etching, as mentioned above, and substituting it by a water bath less invasive with the structural materials. The direct use of a commercial film assures a smooth surface and avoids problems related to its deposition. Furthermore, the thickness of this film is not critical to the manufacturing process because it is used as a sacrificial substrate instead of the classical sacrificial substrate which defines

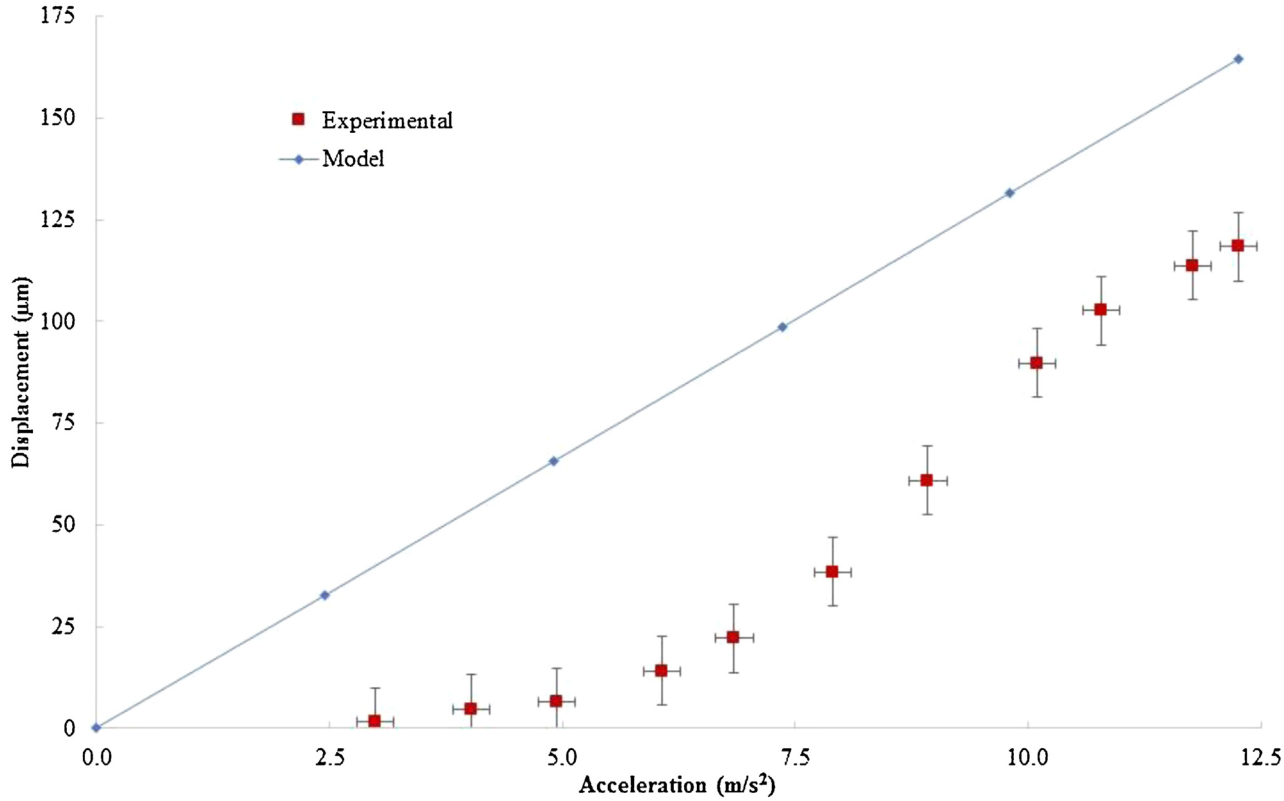

Fig. 5. Cantilever (120 µm gap) peak to peak displacement as a function of acceleration at 10 Hz.

the cantilever gap. In our case, the cantilever gap (or pillar thickness) is directly defined by the number of printed layer by screen printing as well as the mesh density that determines the thickness of one single layer.

The process flow contains 6 steps, as summarized below (Fig. 2):

1. The beam is fabricated using the silver CRSN 2569 ink by screen printing on a PVA film.
2. The pillar is also built by screen printing and aligned with the beam.
3. A layer of adhesive epoxy is deposited by screen printing on top of the pillar.
4. Concurrently, a layer of silver U5603 ink is printed on PET substrate by inkjet printing to define the electrodes. A curing of 1 h at 160 °C is required.

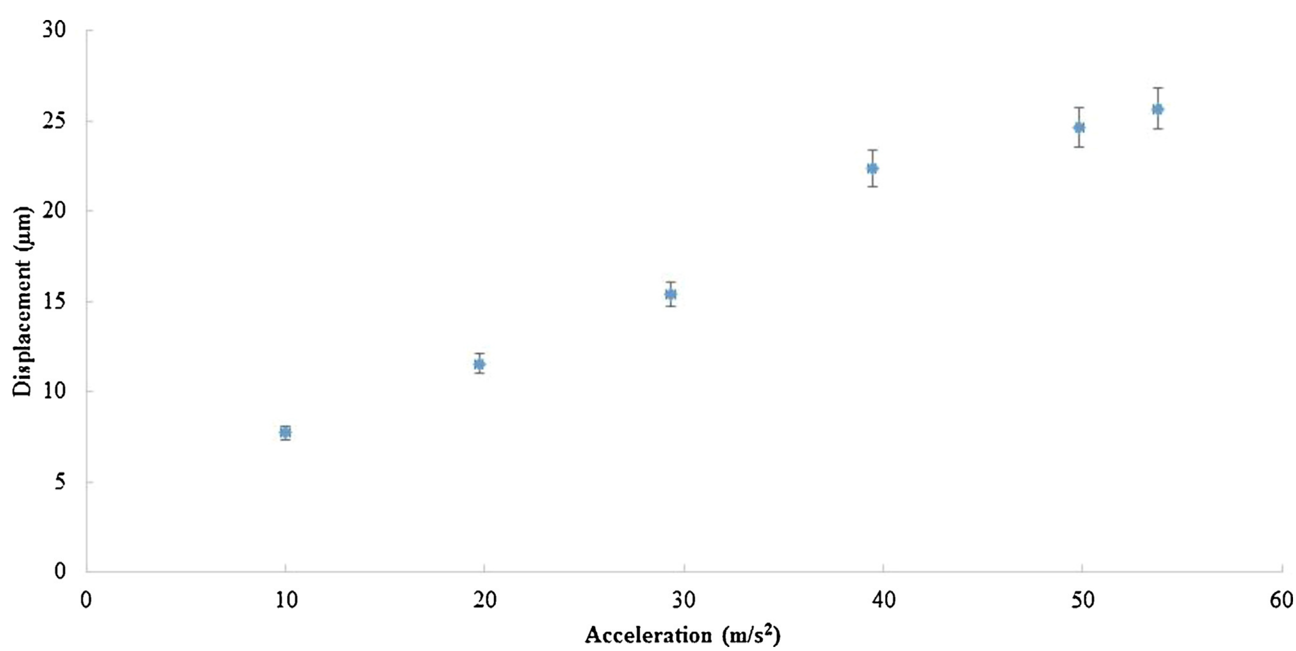

Fig. 6. Cantilever (120 µm gap) peak to peak displacement as a function of acceleration at 25 Hz.

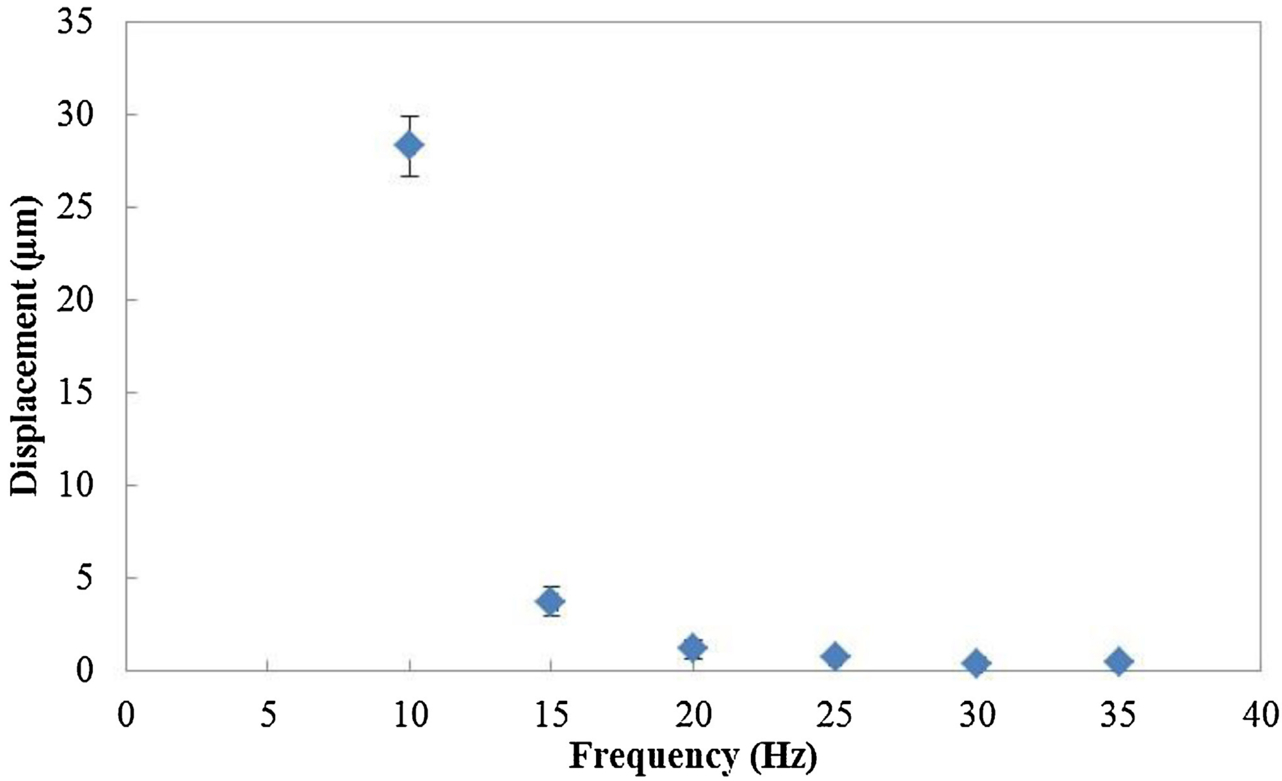

Fig. 7. Cantilever (120 μm gap) peak to peak displacement as a function of frequency at 9.8 m/s^2 acceleration.

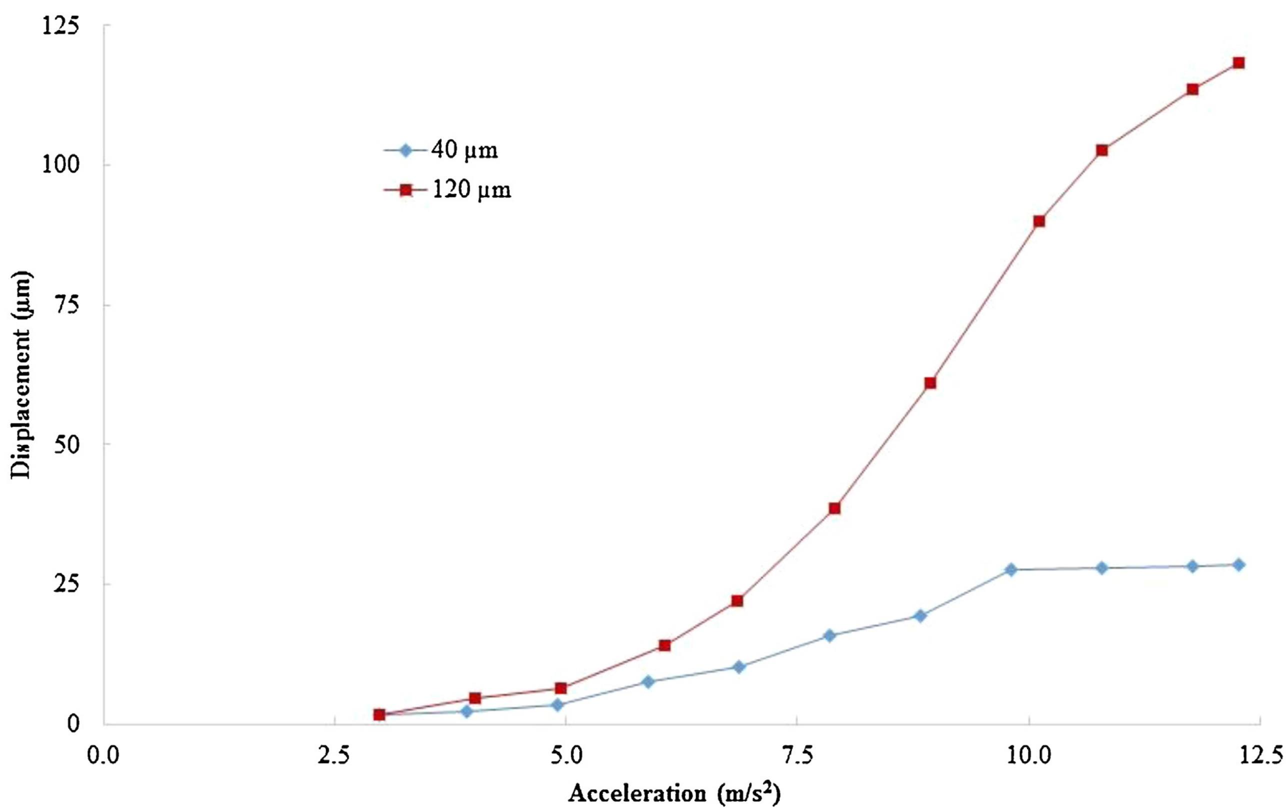

Fig. 8. Cantilevers peak to peak displacement as a function of applied acceleration at 10 Hz.

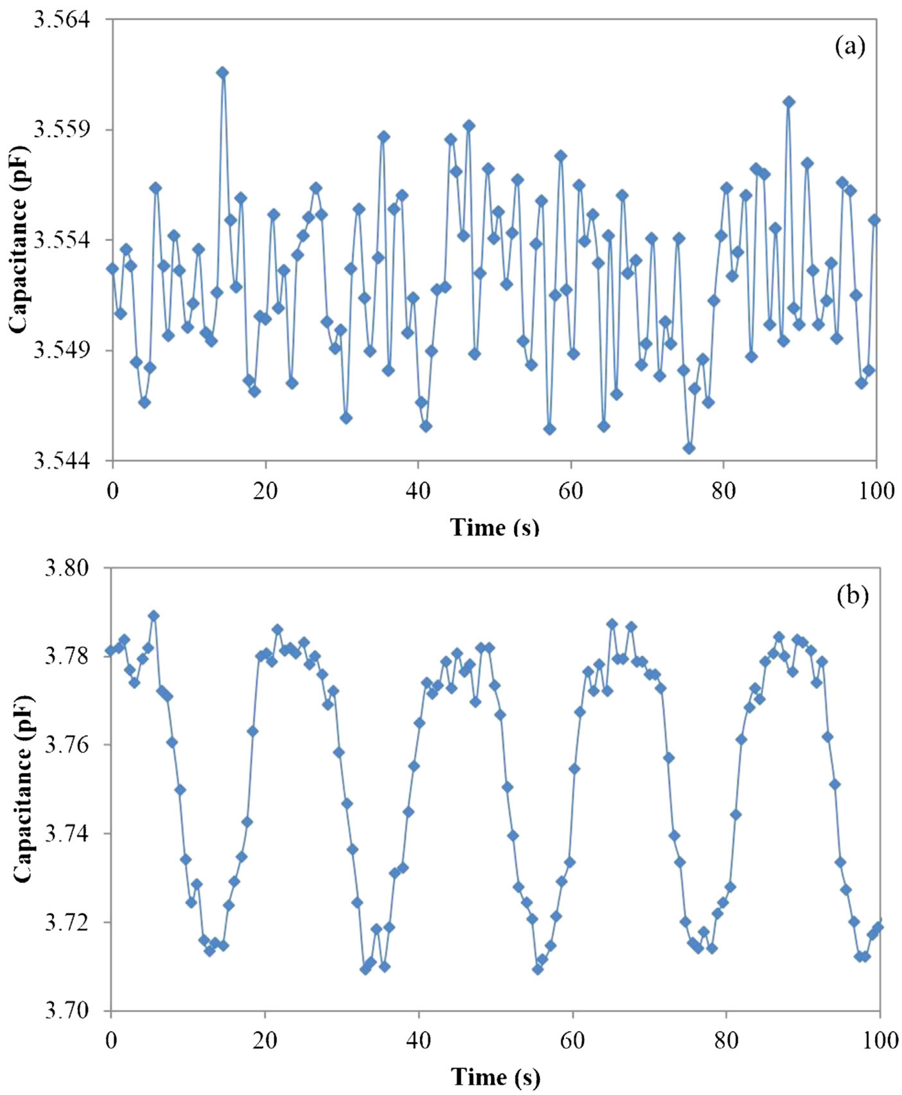

Fig. 9. Capacitance (gap of 120 μm) in time (a) without acceleration (b) with acceleration of 2.9 m/s^2.

5. Then, both PVA and PET substrates are carefully aligned and pasted thanks to the adhesive epoxy H20. A curing of 30 min at 80 °C is needed to harden the adhesive.
6. The final step is to remove the sacrificial substrate. For this purpose, the device is submerged in water at 60 °C during 2 min. The water only removes the PVA without showing etching effects on silver layers.

One of the drawbacks of the manufacturing process of the suspended structure previously developed in [28] was the removal of the substrate layer without interfering the structural layers. Although we have followed the same fabrication process, the solvent used here to remove the sacrificial substrate does not react with silver layers, so that the cantilever flatness is virtually not affected during the release of the sacrificial substrate. As a direct consequence of this, the yield rate is increased by only changing the chosen sacrificial substrate, and additionally both materials, sacrificial substrate and solvent, are biodegradable, which is an advantage in comparison to the previously used ones [33].

A total of 20 replicas have been fabricated following this procedure and only 2 of them were broken. This result shows a preliminary 90% rate of manufacturing success and an increase of 10% compared with the previous strategy based on PMMA sacrificial substrate [28]. The enhancement in manufacturing yield of this improvement of the fabrication process has been verified for the printed suspended cantilevers.

In our previous procedure, we immersed the structure in an acetone bath but we had to take care of the duration of this immersion because if it is longer than 2 min, the acetone started to react with the silver layers. Here, we transfer the cantilever to the substrate thanks to the PVA layer. One of the main advantages of this approach is the enhancement of the quality of the suspended structures. Last and foremost, we avoid the problems related to chemical reactions between the solvents to remove the sacrificial substrate and the structural materials.

2.3. Characterization set-up

The physical characterization of the patterns has been carried out using a Dektak XT^{TM} Stimulus Surface Profiling System (Bruker Corporation, Conventry, UK). The AC electrical characterization for the fabricated cantilevers has been performed by measuring their capacitance and dissipation factor, using the four-wire measurement technique, with a precision Impedance Analyzer 4294A and an impedance probe kit (4294A1) (Agilent Tech., Santa Clara, CA, USA). The calibration method has been described in [34]. The data acquisition and analysis have been automated using Labview software (National Instruments Corporation, Texas, USA).

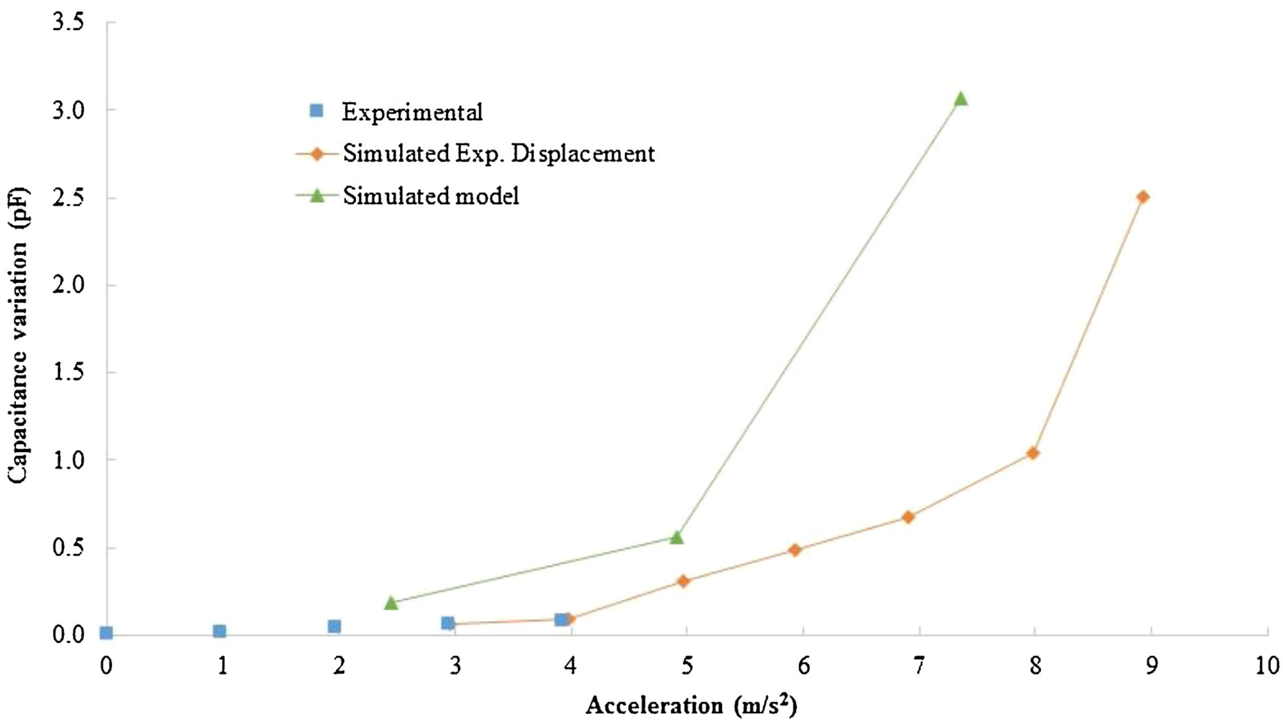

Fig. 10. Variation in capacitance vs applied acceleration at 10 Hz (gap of 120 μm).

The displacement of the cantilevers has been measured with an electrodynamic shaker (Type 4811 Brüel & Kjaer, Naerum, Denmark), an exciter control (Type 1050, Brüel & Kjaer; and Type 2712, Brüel & Kjaer) by applying an oscillation at varying frequency and an acceleration as mechanical input. A laser Doppler vibrometer (LDV) from Polytec (Waldbronn, Germany) has been used to measure the peak-to-peak displacement during the excitation. This set-up has been previously used by Ruan et al. [35] to test piezoelectric cantilevers as harvesters while they are vibrating at a desired frequency and we have already employed it to measure displacement in printed cantilevers [28]. depicts the fabricated suspended structure placed in the set-up for the peak to peak displacement and capacitance measurements.

3. Results and discussion

In this section, we present the results of the physical and electrical characterization of five cantilevers and its comparison with the previous fabricated cantilevers presented in [28]. First, the physical characterization was carried out, showing the reproducibility of this fabrication process. Then, the resistance to different frequencies was studied. Finally, the peak to peak displacement and capacitance were measured and compared with the numerical simulations.

3.1. Physical characterization

After the fabrication, we characterized the dimensions of our devices (Fig. 4), twenty replicas of each cantilever. Table 2 shows the differences between the dimensions measured with a profiling system and the targeted dimensions for these devices. We have also included in Table 2 the dimensions obtained with the fabrication process described in our previous work [28] for comparison purposes. Uncertainties were calculated as one standard deviation of the experimental data. Let us remember that the gap size has been defined being the distance from the substrate to the bottom of the beam (see Fig. 1).

In general, the real dimensions and the targeted ones are similar, the highest difference being found in the cantilever gap. This discrepancy could be caused by the fact that the superposition of several screen printed layers leads to a more homogenous deposition than the single layer case [32]. But this difference (<5%) is lower than the one obtained with the previous proposed method based on PMMA (~10%). Moreover, this cantilever presents a more homogenous surface in terms of beam straightness than the one fabricated on PMMA. In particular, this cantilever only shows a peak to peak displacement at the free end which affects homogenously about 15% the total area of the cantilever. Whereas cantilevers fabricated using PMMA presented peak to peak displacements not only at their free end but also at different locations in the cantilever, the not flat surface represented around 30% the total area of those cantilevers. A flatter surface is achieved now due to the no alteration of silver layers by the water bath to remove the PVA layer. Here, we can also observe a not totally parallel beam to the plan formed by the back electrode, but there is an angle that represents a gap bigger than expected due to this displacement of the beam. This angle is only appreciated at the free end of the beam.

As we have already mentioned, the PVA film tested was 50 μm thick, but the thickness of this layer is not critical. The thickness of the pillar and the beam is directly controlled by the chosen density mesh for the screen printing steps shown in Fig. 2.

3.2. Displacement

First, the peak to peak displacement of the cantilever was measured from 10 Hz to 50 Hz, in steps of 5 Hz. Above 50 Hz, the uncertainty in the peak to peak displacement measurement was too high to differentiate values. In addition to these experiments, the devices were subjected to an acceleration of 9.8 m/s^2 in a frequency range from 10 Hz to 1 kHz without crashing. After this experiment, we measured again the capacitance and peak to peak displacement without noticing any variation in the measurements. As it can be expected due to the fact that structural materials and dimensions are the same, these results are in agreement with those deduced from the frequency behavior of the previous developed cantilevers [28].

The peak to peak displacement at the free end of the cantilever was measured as a function of acceleration at different frequencies. Several experiments were carried out varying the applied acceleration and the frequency of operation. We set the frequencies from 10 Hz to 50 Hz. The range of acceleration varied from 0.98 m/s^2 to 54 m/s^2, depending on the frequency. Fig. 5 shows the peak to peak displacement of the cantilever at 10 Hz. Peak to peak displacements below 2.9 m/s^2 were not possible to measure because the signal noise was comparable to the detected signal. The maximum applied acceleration at 10 Hz with this system was 12 ± 5 m/s^2 (see Fig. 5). In order to know the response for higher acceleration, we set the frequency of oscillation at 25 Hz. At this frequency, the system can achieve acceleration values up to 54 m/s^2 (Fig. 6). The curve obtained at 10 Hz presents a quite linear response ($R^2 = 0.9569$) from about 4.9 m/s^2 to 10.8 m/s^2 and above this value the response shows saturation, whereas the behavior at 25 Hz shows a trend to saturation above 49 m/s^2.

The simulations and experimental results are compared in Fig. 5. There is a quite good agreement between modeled and experimental slope values. The slope obtained with the simulations is 13.45 μm/m/s^2 whereas the one obtained with real data is 13.97 ± 1.02 μm/m/s^2. The slope obtained with this cantilever is more similar to the modeled one than the slope obtained in the previous developed cantilever [28]. In both cases, the linear fits have been calculated from 4.9 m/s^2 to 11.8 m/s^2 because the readout of the peak to peak displacements at lower values of acceleration presented higher variations. The errors have been calculated as the standard deviation of measurements taken from different cantilevers. In the case of the acceleration, errors bars come directly from the error of the measurement set-up.

The dependency between the frequency of work and the peak to peak displacement of the cantilever beam has also been studied (Fig. 7). For this purpose, we measured the displacement at different frequencies for an applied acceleration of 9.8 m/s^2. There is an exponential response with a decay constant of −0.169 μm/Hz. Due to this strong decay with frequency, displacements could not be measured above 50 Hz with enough accuracy to discriminate values. In our previous work the decay constant was smaller (−0.09 μm/Hz), these differences could be related with the non-parallel beam obtained after the acetone bath.

As we mentioned in the design section, we developed the same cantilever with a shorter gap between the suspended structure and the substrate. Fig. 8 displays the peak to peak displacement of both cantilevers at 10 Hz. The short cantilever shows a slope of 3.77 μm/m/s^2 until 9.8 m/s^2 where its response is saturated. Both curves present similar displacements at low acceleration values but around 5.9 m/s^2 the short cantilever evolves slower than the big one. This behavior can be explained by the damping effect which is more appreciable when the gap between the cantilever and the substrate is reduced. The effect of damping is a decreased peak to peak displacement [36,37].

3.3. Capacitance

We measured the change in capacitance induced by the applied acceleration in order to test this device as accelerometer. An array of 201 points containing capacitance values at 10 kHz were read-out out from the impedance analyzer. The beginning of the measurements and vibrations were synchronized through the external trigger mode. In order to ensure the measurements of capacitance versus acceleration, the frequency of work of the shaking setup was set to 10 Hz, the minimum allowed frequency for this set-up.

Fig. 9 shows two different display captures from the measurements taken with the impedance analyzer. There is a parasitic capacitance in parallel with the device of 2.7 pF, which was measured following the same procedure as described in [34]. As can be observed, the peak to peak changes are around 14 fF without acceleration and show a noisy behavior, whereas these variations are about 70–80 fF applying an acceleration of 2.9 m/s^2, showing a clear periodic response.

Due to constraints in the experimental set-up, we were not able to measure changes in capacitance above 3.9 m/s^2. For this reason, we simulated the change in capacitance with the peak to peak displacement obtained experimentally and the simulated one, shown in Fig. 5. These all capacitance variations are depicted in Fig. 10. We have defined the change in the measured capacitance as the difference between the 85th and 15th percentile of the recorded data. As can be observed, the predicted capacitance taking into account the measured peak to peak displacements coincides with the capacitance measured with the impedance analyzer in the whole range of accelerations and similar results in comparison with our previous work are obtained. The mismatch between these data is less than 20 fF.

Looking at the modeled capacitance, the expected change in capacitance is higher than the one obtained with the experimental displacement but both curves show a similar qualitative behavior. The higher the displacement induced, the bigger the capacitance measured. The simulated capacitance from the experimental peak to peak displacements with this fabrication process shows a less noisy curve than the one obtained with the manufacturing process based on PMMA.

4. Conclusions

In this work, we have presented an improvement of a manufacturing process for printed suspended structures that could be used as capacitive pressure or accelerometers. This process is based on a sacrificial substrate, that is to say, the sacrificial layer is located on top of the cantilever beam instead of between the beam and its support layer. These cantilevers have been fabricated by screen printing on PET providing more flexibility to the final application. Although this procedure was already proved using silver layer as structural material and PMMA as sacrificial substrate, the failure rate was higher and the resulting beams were not totally flat beam. These imperfections were caused during the removal of the sacrificial substrate due to the fact that the solvent partially reacted with the silver layer. We have faced these inconveniences by substituting the sacrificial material. Concretely, we have used PVA that can be dissolved in water instead of acetone. Thanks to this material, we have increased the manufacturing yield as well as the flatness of the beam. In addition to this, the process is more environmental-friendly with the use of biodegradable materials. Finally, we have characterized the peak to peak displacement of these cantilevers comparing and contrasting their results with the previous developed structures.

The behaviour of this cantilever is quite similar in terms of displacement and capacitance to the previous one [28] but with the advantage of higher manufacturing yield and straighter surface compared with the previous manufacturing process developed. In addition, we have shown the fabrication of two cantilevers that only differ in the gap thickness. This difference is only caused by the number of printed layer for the pillar during the fabrication process. This result shows that the thickness of the pillar can be directly controlled by the number of printed layers. Obviously, the cantilever dimensions can be controlled by only changing the screen.

Acknowledgments

This work was partially funded by Spanish Ministerio de Economía y Competitividad under Project CTQ2013-44545-R, the Junta de Andalucía, Spain (Proyecto de Excelencia P10-TIC-5997) and Project, CEI BioTIC CEI-2013-P-2. These projects were partially supported by European Regional Development Funds (ERDF). We thank EnviroMEMS research group (Sensors, Actuators and Microsystems Laboratory, École Polytechnique Fédérale de Lausanne, Switzerland) headed by Dr. Briand, for sharing its experimental setup and discussing the results.

References

[1] H. Lang, M. Baller, R. Berger, C. Gerber, J. Gimzewski, F. Battiston, et al., An artificial nose based on a micromechanical cantilever array, Anal. Chim. Acta 393 (1999) 59–65.
[2] H. Baltes, O. Brand, A. Hierlemann, D. Lange, C. Hagleitner, CMOS MEMS-present and future, micro electro mechanical systems, 2002 The Fifteenth IEEE International Conference on, IEEE (2002) 459–466.
[3] K. Suganuma, Introduction to printed electronics, Springer Science & Business Media, 2014.
[4] D. Briand, A. Oprea, J. Courbat, N. Bârsan, Making environmental sensors on plastic foil, Mater. Today 14 (2011) 416–423.
[5] H.W. Choi, T. Zhou, M. Singh, G.E. Jabbour, Recent developments and directions in printed nanomaterials, Nanoscale 7 (2015) 3338–3355.
[6] N. Serra, Epoxy-graphite resistive composites: formulation, characterization and applications, École Polytechnique Fédérale de Lausanne (2012).
[7] E. Lam, H. Li, M. Schmidt, Silver nanoparticle structures realized by digital surface micromachining, International solid-state sensors, Actuators and Microsystems Conference, 2009 TRANSDUCERS, IEEE (2009) 1698–1701.
[8] E. Park, J. Jeon, V. Subramanian, T.-J. Liu, Inkjet-printed microshell encapsulation: a new zero-level packaging technology, IEEE 25th International Conference on Micro Electro Mechanical Systems (MEMS) (2012) 357–360.
[9] E.S. Park, Y. Chen, T.-J.K. Liu, V. Subramanian, Inkjet-printed micro-electro-mechanical switches, IEEE International Electron Devices Meeting (IEDM), IEEE (2011) 2–29.
[10] S. Chung, M.A. Ul Karim, H.-J. Kwon, V. Subramanian, High-performance inkjet-printed four-terminal microelectromechanical relays and inverters, Nano Lett. 15 (2015) 3261–3266.
[11] C. Castille, I. Dufour, C. Lucat, Longitudinal vibration mode of piezoelectric thick-film cantilever-based sensors in liquid media, Appl. Phys. Lett. 96 (2010) 154102–154103.
[12] H. Debéda, P. Clément, E. Llobet, C. Lucat, One-step firing for electroded PZT thick films applied to MEMS, Smart Mater. Struct. 24 (2015) 025020.
[13] N. Serra, T. Maeder, O. Gentsch, P. Ryser, Fabrication of polymer-based micro devices: formulation and study of the paste, Sens. Actuators A Phys. 172 (2011) 336–340.
[14] F. Molina-Lopez, D. Briand, N.F. de Rooij, Large arrays of inkjet-printed MEMS microbridges on foil, IEEE 27th International Conference on Micro Electro Mechanical Systems (MEMS), IEEE (2014) 506–509.
[15] R. Shankar, W. Cross, J. Kellar, K. Whites, D. Anagnostou, Advances in direct-write printing of RF-MEMS using M3D, Microwave Symposium (IMS), 2014, IEEE MTT-S International, IEEE (2014) 1–4.
[16] S.B. Fuller, E.J. Wilhelm, J.M. Jacobson, Ink-jet printed nanoparticle microelectromechanical systems, J. Microelectromech. Syst. 11 (2002) 54–60.
[17] Y. Wei, R. Torah, K. Yang, S. Beeby, J. Tudor, A novel fabrication process to release a valveless micropump on a flexible substrate, Smart Mater. Struct. 23 (2014) 025034.
[18] Y. Wei, R. Torah, K. Yang, S. Beeby, J. Tudor, Screen printing of a capacitive cantilever-based motion sensor on fabric using a novel sacrificial layer process for smart fabric applications, Meas. Sci. Technol. 24 (2013) 075104.
[19] Y. Wei, R. Torah, K. Yang, S. Beeby, J. Tudor, A novel fabrication process for capacitive cantilever structures for smart fabric applications, Design, Test, Integration and Packaging of MEMS/MOEMS (DTIP), 2012 Symposium on, IEEE (2012) 136–139.
[20] Y. Wei, R. Torah, K. Yang, S. Beeby, J. Tudor, A novel fabrication process to realise piezoelectric cantilever structures for smart fabric sensor applications, IEEE, Sensors, IEEE (2012) 1–4.
[21] Y. Wei, R. Torah, K. Yang, S. Beeby, J. Tudor, Screen printed capacitive free-standing cantilever beams used as a motion detector for wearable sensors, Procedia Eng. 47 (2012) 165–169.
[22] R. Lakhmi, H. Debéda, I. Dufour, C. Lucat, Force sensors based on screen-printed cantilevers, IEEE Sens. J. 10 (2010) 1133–1137.
[23] R. Lakhmi, H. Debeda, M. Maglione, I. Dufour, C. Lucat, Study of screen-printed PZT cantilevers both self-actuated and self-read-out, Int. J. Appl. Ceram. Technol. 11 (2013) 311–320.
[24] C. Lucat, P. Ginet, C. Castille, H. Debéda, F. Ménil, Microsystems elements based on free-standing thick-films made with a new sacrificial layer process, Microelectron. Reliab. 48 (2008) 872–875.
[25] S. Nakano, T. Sekitani, T. Yokota, T. Someya, Low operation voltage of inkjet-printed plastic sheet-type micromechanical switches, Appl. Phys. Lett. 92 (2008) 053302–053303.
[26] T. Yokota, S. Nakano, T. Sekitani, T. Someya, Plastic complementary microelectromechanical switches, Appl. Phys. Lett. 93 (2008) 023305.
[27] M. Ataka, M. Mita, H. Toshiyoshi, H. Fujita, Electrostatic microactuators in a flexible sheet—smart MEMS, 17th International Conference on Solid-State Sensors, Actuators and Microsystems (TRANSDUCERS & EUROSENSORS XXVII), IEEE (2013) 2341–2344.
[28] A. Rivadeneyra, J. Fernández-Salmerón, M. Agudo-Acemel, A.J. Palma, L.F. Capitan-Vallvey, J.A. López-Villanueva, Cantilever fabrication by a printing and bonding process, J. Microelectromech. Syst. 24 (2014) 880–886.
[29] B. Aspar, Characterization of SOI substrates: application to recent SIMOX and UNIBOND wafers, Electrochemical Society Proceedings (1996) 99–111.
[30] A. Rivadeneyra, J.A. Lopez-Villanueva, R. O'Keeffe, N. Jackson, M. O'Neill, A. Mathewson, Frequency response of variants of a cantilever beam, synthesis, modeling, analysis and simulation methods and applications to circuit design (SMACD), 2012 International Conference on, IEEE (2012) 177–180.
[31] M. Emam, Finite Element Analysis of Composite Piezoelectric Beam Using Comsol, Drexel University, 2008.
[32] J.F. Salmerón, F. Molina-Lopez, D. Briand, J.J. Ruan, A. Rivadeneyra, M.A. Carvajal, et al., Properties and printability of inkjet and screen-printed silver patterns for RFID antennas, J. Electron. Mater. 43 (2014) 604–617.
[33] S. Matsumura, K. Toshima, Biodegradation of poly(vinyl alcohol) and vinyl alcohol block as biodegradable segment, hydrogels and biodegradable polymers for bioapplications, Am. Chem. Soc. (1996) 137–148.
[34] A. Rivadeneyra, J. Fernández-Salmerón, M. Agudo, J. López-Villanueva, L. Capitan-Vallvey, A. Palma, Design and characterization of a low thermal drift capacitive humidity sensor by inkjet-printing, Sens. Actuators B Chem. 195 (2014) 123–131.
[35] J.J. Ruan, R.A. Lockhart, P. Janphuang, A.V. Quintero, D. Briand, N. de Rooij, An automatic test bench for complete characterization of vibration-energy harvesters, IEEE Trans. Instrum. Meas. 62 (2013) 2966–2973.
[36] W. Choi, Y. Jeon, J.-H. Jeong, R. Sood, S.-G. Kim, Energy harvesting MEMS device based on thin film piezoelectric cantilevers, J. Electroceram. 17 (2006) 543–548.
[37] X.X. Zhang, S.J. Peng, J.L. Zou, Air damping effects of MEMS parallel-plate structure using ANSYS thin film analysis, Adv. Mater. Res. 403 (2012) 4588–4592.

Biographies

Almudena Rivadeneyra Torres completed her five years degrees in telecommunication engineering (2009), environmental sciences (2009) and electronics engineering (2012), at the University of Granada (Spain) with exchange at Technische Universität Berlin. She received the master degree in computer and network engineering in 2010. In 2014, she received her Ph.D. in design and development of environmental sensors in the University of Granada. Currently, she is postdoctoral researcher in the Nanoelectronics Institute of the Technische Universität München.

José Fernández Salmerón was born in Granada, Spain, on April 28, 1985. He completed the major degrees in telecommunication engineering and electronics engineering in 2009 and 2011, respectively, at the University of Granada (Spain) with exchange at Technische Universität Berlin. He obtained the master degree in computer and network engineering in 2012. He obtained his Ph.D. in development of sensing capabilities in RFID technologies in 2014 in the University of Granada. At present, he is enrolled as postdoctoral researcher in the Nanoelectronics Institute of the Technische Universität where he is involved in a European project on the design and development of smart RFID labels with sensing capabilities.

Manuel Agudo Acemel, received his Higher Technician in Graphics Arts Production and design title in the Audiovisual & Graphic Training Centre Puerta Bonita in Madrid, 2002–2005. He graduated in Multimedia degree at the University Oberta of Catalunya in 2014. From 2006 to 2011 his main issue interests are focus on different applications in the graphics arts industry like packaging and research of materials for its production. Since 2011 he works on Chemicals and Electronic sensors development through diverse Graphics techniques at the University of Granada.

Juan A. López-Villanueva received a PhD in Physics in 1990 from the University of Granada, Spain, where he is presently a Full Professor of Electronic Technology. His research explores electron device physics, modelling and characterization. His current interest also involves devices and systems for energy generation and storage.

Luis Fermín Capitan-Vallvey, Full Professor of Analytical Chemistry at the University of Granada, received his B.Sc. in Chemistry (1973) and Ph.D. in Chemistry (1986) from the Faculty of Sciences, University of Granada (Spain). In 1983, he founded the Solid Phase Spectrometry group (GSB) and in 2000, together with Prof. Palma López, the interdisciplinary group ECsens, which includes Chemists, Physicists and Electrical and Computer Engineers at the University of Granada. His current research interests are the design, development and fabrication of sensors and portable instrumentation for environmental, health and food analysis and monitoring.

Alberto J. Palma was born in 1968 in Granada (Spain). He received the BS and M.Sc. degrees in physics in 1991 and the Ph.D. degree in 1995 from the University of Granada, Granada, Spain. He is currently full professor with the University of Granada in the Department of Electronics and Computer Technology. Since 1992, he has been working on trapping of carriers in different electronic devices (diodes and MOS transistors) including characterization and simulation of capture cross sections, random telegraph noise, and generation-recombination noise in devices. From 2000 in the interdisciplinary group ECsens, his current research interests are devoted to design, development and fabrication of sensors and portable electronic instrumentation for environmental, biomedical and food analysis and monitoring. Recently we are working in printing sensors on flexible substrates with processing electronics using inkjet and screen printing technologies.